

# Tillage and water erosion on different landscapes in the northern North American Great Plains evaluated using $^{137}\text{Cs}$ technique and soil erosion models

Sheng Li <sup>a</sup>, David A. Lobb <sup>a,\*</sup>, Michael J. Lindstrom <sup>b,1</sup>, Annemieke Farenhorst <sup>a</sup>

<sup>a</sup> Department of Soil Science, University of Manitoba, Canada

<sup>b</sup> USDA-ARS, Morris, Minnesota, USA

Received 19 June 2006; received in revised form 10 December 2006; accepted 18 December 2006

## Abstract

Total soil erosion is the integrated result of all forms of soil erosion — wind, water and tillage. It has been recognized that in topographically complex landscapes, individual soil erosion processes and their interactions all contribute towards total soil erosion. In this study, two field sites, representing different landscapes in the northern region of the North American Great Plains, were examined. Water and tillage erosions were estimated using the established water and tillage erosion models and total soil erosion was estimated using the  $^{137}\text{Cs}$  technique.

We determined that the patterns of water and tillage erosion across the landscapes are mainly dependent on topographic features and they are fundamentally different within topographically complex landscapes. On the slope of undulating landscapes, tillage and water erosion both contribute considerably to total soil erosion. On the knoll of hummocky landscapes, tillage erosion dominates the pattern of total soil erosion. Tested against the Cs measurements, the patterns of total soil erosion cannot be well estimated by water or tillage erosion model alone unless one of the two erosion processes predominate over the other erosion processes. Combining water and tillage erosion models generally provides better estimations of total soil erosion than the component models on their own. Most soil properties and crop yield were found to be closely correlated with total soil erosion. For a given erosion process, the soil erosion patterns estimated using different models with reasonable parameter settings were similar to each other. However, it is necessary to choose an optimal model and to obtain accurate parameters for the purpose of accurate assessments of the erosion rates.

© 2007 Elsevier B.V. All rights reserved.

*Keywords:* Tillage erosion; Water erosion; Total soil erosion; Northern North American Great Plains

## 1. Introduction

Soil erosion affects both soil properties and soil processes, and is widely recognized as a major cause of soil degradation in arable land. Historically, water and wind erosions were assumed to be the major forms of soil erosion. Since the “rediscovery” of tillage erosion in the 1990s, field evidence from different parts of the world has shown that tillage erosion is another major form of soil erosion (e.g. Lindstrom et al., 1990, 1992; Govers et al., 1994; Lobb et al., 1995). Each soil erosion process has its

characteristic pattern across the landscape and each will contribute to some degree to the total soil erosion evident within a field (Van Oost et al., 2000; De Alba et al., 2004; Papiernik et al., 2005). For example, water erosion mainly causes soil loss on mid-slopes while tillage erosion mainly causes soil loss on hilltops. The pattern of total soil erosion is complicated due to the linkages and interactions between the erosion processes. Linkages refer to the simple additive effects between different erosion processes. Interactions occur when one erosion process changes the erodibility of the landscape for another erosion process or when one process works as a delivery mechanism for another erosion process (Lobb, 1991; Lobb et al., 2003). For a given set of conditions, especially in topographically complex landscapes, the observed soil redistribution pattern in agricultural land is an integrated result of all forms of soil erosion,

\* Corresponding author. Tel.: +1 204 474 9319; fax: +1 204 474 7642.

E-mail address: [lobbda@ms.umanitoba.ca](mailto:lobbda@ms.umanitoba.ca) (D.A. Lobb).

<sup>1</sup> Retired.

including the contributions of individual erosion processes and the interactions between different erosion processes.

Soil erosion can be assessed through modeling or field measurement (Heuvelink et al., 2006). The modeling approach is based on the knowledge of the erosion processes and/or how various factors influence the erosion processes. Due to the complexity of the individual erosion processes, researchers usually deal with each soil erosion process independently and developed various models for each erosion process. For example, the Revised Universal Soil Loss Equation (RUSLE) and the Water Erosion Prediction Project (WEPP) are widely used to estimate water erosion (Flanagan and Nearing, 1995; Renard et al., 2001) and more recently, tillage erosion models have been developed and used to estimate tillage erosion (e.g. Lobb and Kachanoski, 1999).

The accuracy of the model-estimated soil erosion is limited for two reasons. Firstly, there are high uncertainties associated with the erosion models. Soil erosion, especially water erosion, is inherent with large spatial and temporal variability. It is always a dilemma for modeling workers to decide whether to use a simple-structure model or to use a complex-structure model (e.g. RUSLE versus WEPP for water erosion). In a simple-structure model, the erosion process is characterized by a few key parameters and/or functions and, inevitably, some delicate but in some cases, important aspects of the process are neglected. In a complex-structure model, the erosion process is simulated more completely, however, the parameterization is often difficult (Heuvelink et al., 2006). In either case, there are high uncertainties associated with the model results. Jetten et al. (2003) examined different water erosion models and found that when compared to field measurements, uncalibrated model results are generally bad and the simple-structure models perform equally well as the complex-structure models. Secondly, the linkages and/or interactions between different erosion processes are often overlooked. It is a common practice in soil erosion studies to focus on one predominant erosion process by assuming that other erosion processes are negligible. This assumption is questionable in some landscapes where more than one erosion process contributes substantially to total soil erosion. It has been shown that improvements could be made by combining water and tillage erosion models (Schumacher et al., 1999; Van Oost et al., 2000; Papiernik et al., 2005).

Field measurement provides another approach to assess soil erosion. The  $^{137}\text{Cs}$  technique is a commonly used tool. The  $^{137}\text{Cs}$ -estimated soil erosion includes soil erosion by all forms of soil erosion processes and their interactions. Although the accuracy of  $^{137}\text{Cs}$  estimates is restricted by the assumption of a spatially uniform distribution of the initial  $^{137}\text{Cs}$  level and by the reliability of the conversion model, the  $^{137}\text{Cs}$  technique has been successfully used worldwide in soil erosion studies (e.g. de Jong et al., 1983; Quine et al., 1997; Lobb et al., 1999; Pennock, 2003). By comparing the model estimates to the  $^{137}\text{Cs}$  estimates, it is possible to evaluate the contributions of different erosion processes to the total soil erosion.

Due to the geological youth of the landscape and the relatively short cultivation history, soil-landscapes in the northern region of the North American Great Plains (northern NAGP) are

generally more complex than those in Europe and Asia. More than 75% of the agricultural land in this region is classified as hilly (rolling, undulating and hummocky) landscapes. Both water and tillage erosion have been reported to contribute to the total soil erosion in the northern NAGP (Pennock, 2003; De Alba et al., 2004; Papiernik et al., 2005; Schumacher et al., 2005). It is important to examine both erosion processes, their linkages and interactions because the redistribution of soil mass causes the variability of soil properties across the landscape and, therefore, influences other landscape-driven soil processes such as water contamination, pesticide fate and greenhouse gas emission. For example, Pennock and Corre (2001) found that both soil organic carbon (SOC) storage and  $\text{N}_2\text{O}$  emissions are controlled by the predominant water or soil redistribution processes occurring in different landform elements.

The objectives of this study are: 1) to estimate water, tillage and total soil erosion on topographically complex landscapes; 2) to compare the relative contributions of water and tillage erosion to total soil erosion on different landscapes; 3) to investigate the effects of water, tillage and total soil erosion on soil properties and crop yield; and 4) to examine the errors and uncertainties associated with different erosion models and the  $^{137}\text{Cs}$  technique.

## 2. Materials and methods

### 2.1. Study sites and laboratory analysis

Two field sites were examined in this study. The first site is a 2.7 ha portion of a 16 ha field near the town of Cyrus, in west central Minnesota, USA. The sampling area features a trough in the western part, a knoll in the middle and a slightly concave slope towards the eastern side of the field (Fig. 1). The second site is a 0.8 ha portion of a 42 ha field near the town of Deerwood, in south-western Manitoba, Canada. The sampling area is a complex of small knolls (Fig. 2). The central part of this area is a depression, which gives it a bowl shape. The two sites are typical of the landscapes in the northern NAGP: the slope of an undulating landscape (the Cyrus site) and the knoll of a hummocky landscape (the Deerwood site). A general overview of the field sites and the associated tillage and cropping systems employed at each site are summarized in Table 1.

The background field information, and the collection and processing of soil samples (except for  $^{137}\text{Cs}$  radioactivity) at the Cyrus site were described in De Alba et al. (2004) and, Papiernik et al. (2005). To summarize, depth-incremental soil samples down to C horizon were collected at 288 points on a  $10 \times 10$  m grid. Each sampling location was surveyed using a Trimble AgGPS-132 system. Soil samples were air-dried, sieved through a 2-mm screen, and both soil and stone fractions were weighed. The surface samples (0–15 cm) were analyzed for soil dry bulk density ( $\rho$ ), stone content ( $C_{\text{St}}$ ), soil organic carbon content ( $C_{\text{OC}}$ ), total carbonates content ( $C_{\text{IC}}$ ) and pH. Soil dry bulk density and stone content were calculated from the mass of the soil and the stones. For the soil organic carbon content analyses, inorganic carbon was removed by digestion with 6 M HCl followed dry combustion of 0.12 g oven-dried

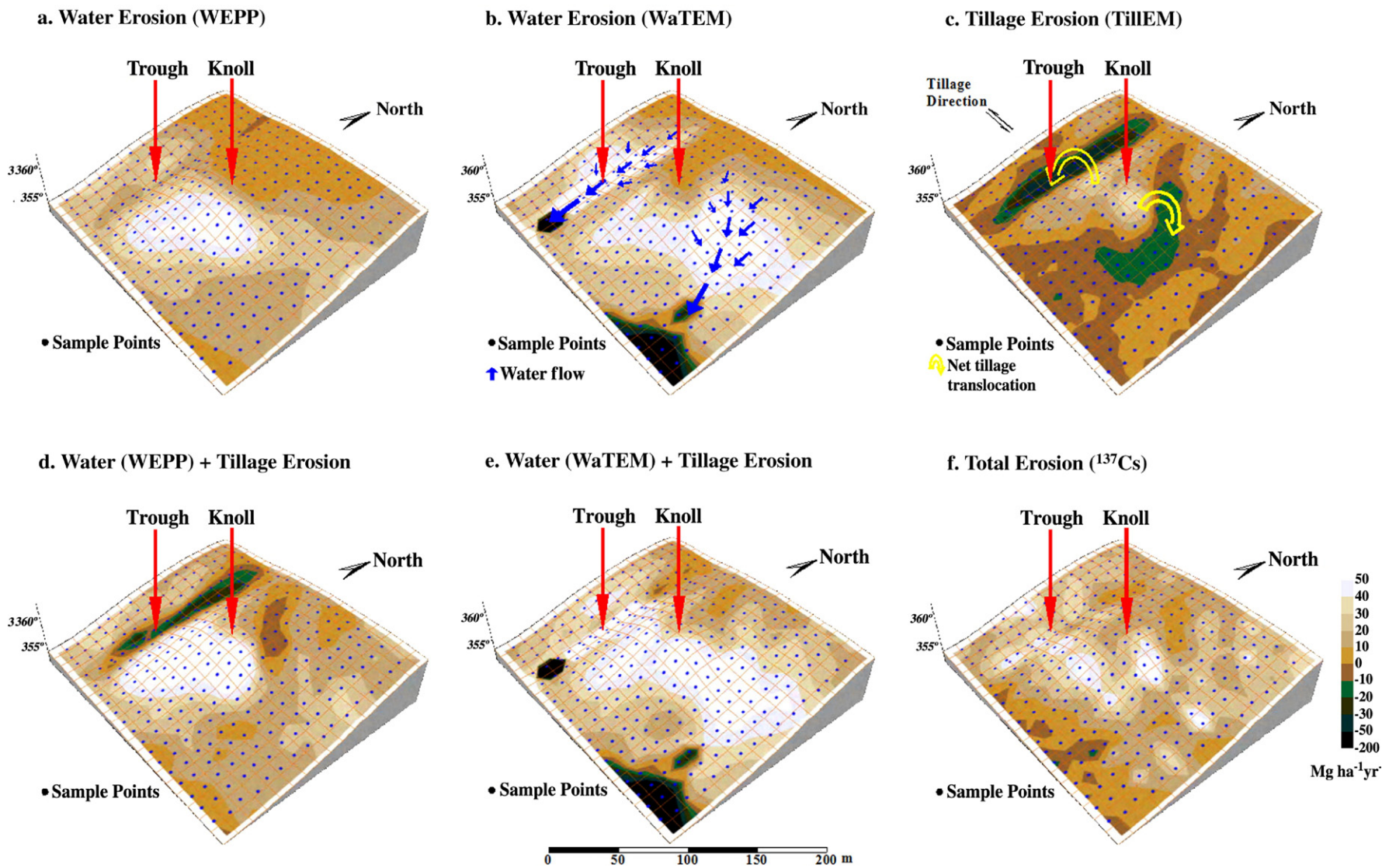


Fig. 1. Estimated a. water (WEPP), b. water (WaTEM), c. tillage (Tillem), d. water (WEPP)+tillage, e. water (WaTEM)+tillage, and f. total ( $^{137}\text{Cs}$ ) soil erosion at the Cyrus site.

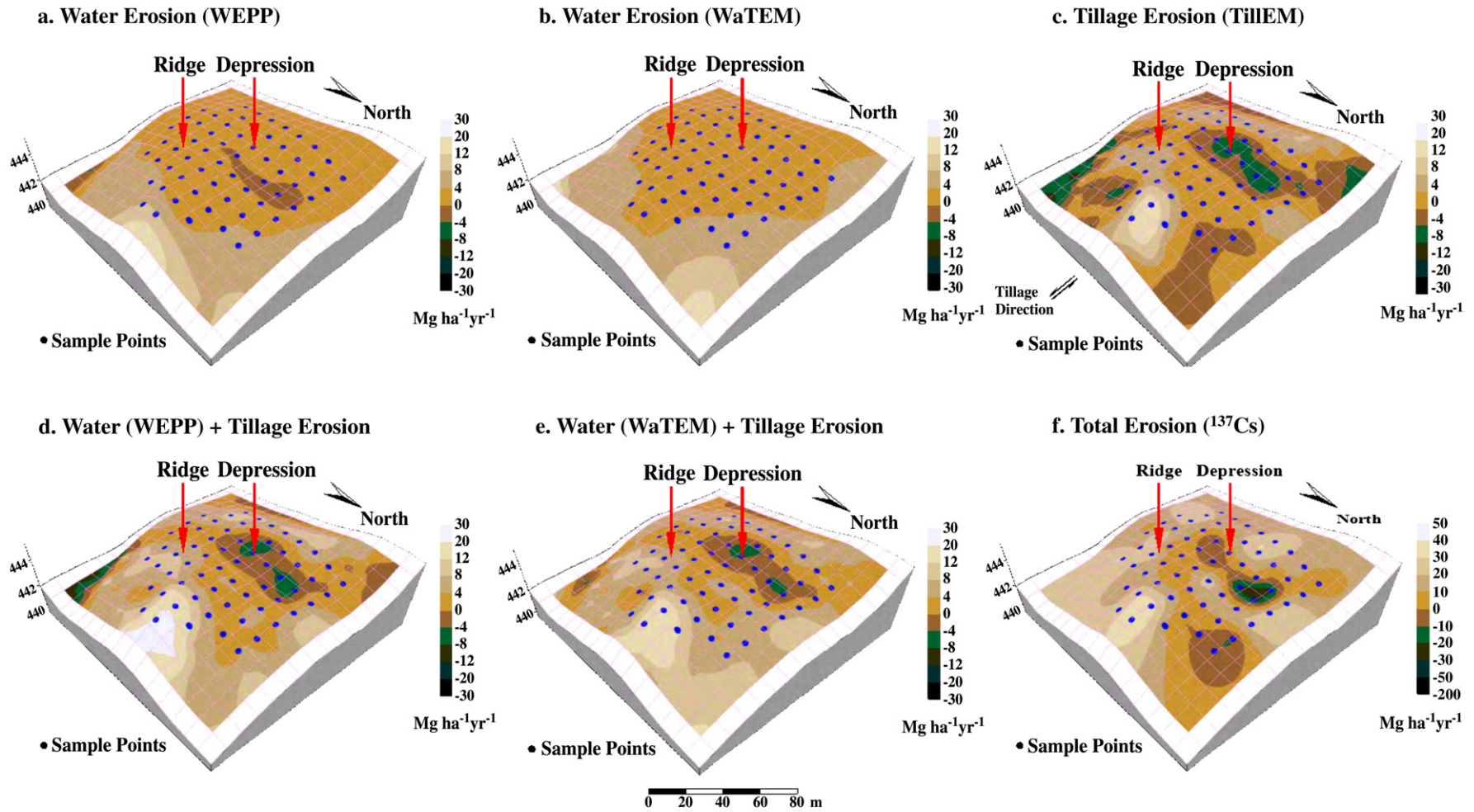


Fig. 2. Estimated a. water (WEPP), b. water (WaTEM), c. tillage (Tillem), d. water (WEPP)+tillage, e. water (WaTEM)+tillage, and f. total ( $^{137}\text{Cs}$ ) soil erosion at the Deerwood site.

Table 1  
Characteristics of the field sites

	Cyrus site	Deerwood site
Location	Minnesota, USA	Manitoba, Canada
Coordinates	45.67° N, -95.75° E	49.35° N, -98.35° E
Soil texture of the Ap horizon <sup>a</sup>	Loam	Sandy loam
Annual precipitation	595 mm	567 mm
Crops	Corn, winter wheat, soybean	Winter wheat, oat, canola
Major tillage implements	Mouldboard plough tandem disc	Heavy cultivator light cultivator

<sup>a</sup> Of the sampling area not of the whole field.

soil using a LECO model CHN 600 C and N determinator (Nelson and Sommers, 1982). Carbonate content was determined using a volumetric calcimeter that measures evolved carbon dioxide upon addition of 6 M HCl-FeCl<sub>2</sub> to a soil sample (Loeppert and Suarez, 1996). Soil pH values were obtained using 10 ml of 0.01 M CaCl<sub>2</sub> and 5 g air-dried soil (McKeague, 1978).

<sup>137</sup>Cs radioactivity was detected at 662 keV using Broad Energy Germanium Gamma spectrometers (Canberra BE3830, Landscape Dynamics Laboratory, University of Manitoba, Canada) with counting time ranging from 4 to 12 h, providing a detection error < 10%. <sup>137</sup>Cs inventory at a given sample point was determined by the summation of area-based <sup>137</sup>Cs radioactivities of all the samples taken from different layers at this given point. A reference site was established on a native grassland adjacent to the Cyrus field site. At the reference site, seven soil cores were taken in 2-cm depth increments to one meter. The profile <sup>137</sup>Cs radioactivity was examined and the inventory was used as the reference <sup>137</sup>Cs level for the Cyrus site (2093 Bq m<sup>2</sup>).

Crop yields (wheat in 2000, 2001 and 2003 and soybean in 2002) at each sampling point were determined by harvesting a 13 m<sup>2</sup> area with the sampling point located in the center of the area. Yields were averaged across years to determine the average crop yield (*Y*) at each sample point.

For the Deerwood site, detailed field information can be found in Li et al. (in press). Depth-incremental soil samples were collected at 63 points on a 10 × 10 m grid. Each sampling location was surveyed using a Total Station (Sokkia set 4110) and georeferenced using a Trimble TSC1 GPS system. The depth of Ap horizon (*D*) was determined in the field by a pedologist. The procedures for the determinations of soil dry bulk density, stone content and <sup>137</sup>Cs inventory were the same as those used at the Cyrus site. The reference <sup>137</sup>Cs level (2060 Bq m<sup>-2</sup>) was determined based on the average <sup>137</sup>Cs inventory of the samples taken from three sites located within 10 km of the study area (two pasture sites and one old farm yard site).

Soil samples of the Cyrus were collected in August, 2000 and those of the Deerwood sites were collected in October, 2002. January 1, 2002 was used as the reference date of <sup>137</sup>Cs radioactivity.

The topographic data of the two sites were used to generate Digital Elevation Models (DEM, 10 m and 8 m spacing for the

Cyrus and the Deerwood site, respectively) by using GS+ 5.1.1<sup>®</sup> point kriging interpolation. The DEMs were used as the topographic input data for the water and tillage erosion models.

## 2.2. Water erosion — WEPP and WaTEM

Two established models, WEPP (2002 Hillslope version) and the water erosion component of the Water and Tillage Erosion Model (WaTEM, Van Oost et al., 2000), were used to estimate water erosion.

WEPP is a two-dimensional model and calculates point-water-erosion rates along a two-dimensional slope (Flanagan and Nearing, 1995). To simulate water erosion in three-dimensions, WEPP was run on both North–South and East–West oriented transects in the DEMs. As required by WEPP, transects were divided into sub-slopes at the summit and/or nadir points to ensure there was no negative slope gradient point. In total, 67 and 55 sub-slopes were generated for the Cyrus and the Deerwood sites, respectively. For a given point, this procedure tracked water flows from two perpendicular directions, and therefore, to some degree, it took into account the effect of convergent and divergent water flows. In addition, this procedure accounted for the directionality of water erosion caused by cropping and tillage, i.e. water flows along the furrows created by tillage operations and crop rows rather than the direction of the steepest slope (Desmet and Govers, 1997; Takken et al., 2001).

The climate data necessary for WEPP were generated using the CLIGEN v. 5.2 program incorporated in WEPP. For the Cyrus site, the Morris MN climate station data was used and the simulated 46 yr mean annual precipitation was 594 mm. For the Deerwood site, linear interpolation of the data from the two closest climate stations in the USA (Edmore ND and Grafton ND, located about 100–125 km away from the site) was used and the simulated 48 yr mean annual precipitation was 422 mm. Management data were generated based on the cropping history and the current tillage practices employed at the two sites (Table 1, detailed data not shown). For the Cyrus site, the dominant soil SVEA (Loam) was used. For the Deerwood site, soil data were generated based on the measurements of the soil samples (soil texture is sandy loam). Single soil types were used on both sites for the simplification of the modeling.

The WEPP program was run for 46 and 48 iterations (representing 46 and 48 yrs) to match the duration of <sup>137</sup>Cs fallout (from 1954 to 2000 and to 2002) at the Cyrus site and the Deerwood site, respectively. The output point-water-erosion rates (100 points per slope) were regrouped into the DEM transects and were averaged so that the water erosion rates on the grid nodes of the DEMs represented the average water erosion rates of the respective sections (length=DEM spacing). Each individual grid node had two values, calculated from the North–South transect and the East–West transect, and the sum of these two values was the water erosion rate assigned to this grid node.

To compare the two sites and to isolate the effect of topography, WEPP was run for a second time on the Deerwood site

using the Cyrus site's climate, management and soil data. This reanalysis was also performed, because: 1) heavier implements, similar to those used on the Cyrus site, had previously been used on the Deerwood site during the early-1950s to the late-1980s; and 2) the recorded local annual precipitation on the Deerwood site (567 mm, Table 1) is considerably greater (about 30–65 mm) than those of the other climate stations in southwestern Manitoba, Canada (Environment Canada, 2006) and greater than the simulated annual precipitation (422 mm). This indicates that using the coarse scale climate data in the WEPP database might have considerably underestimated the local precipitation at the Deerwood site.

The water erosion component of WaTEM is a three-dimensional model based on RUSLE but incorporates routing algorithms to simulate both convergent and divergent water flows (Van Oost et al., 2000). At both sites, The “Govers- (1991)” routing algorithm was used, and the Transport Capacity Coefficient ( $k_{TC}$ ) was assumed to be 170 m. Additional parameter settings for the Cyrus site were based on Papiernik et al. (2005) and included: 1) a rainfall-runoff erosivity factor ( $R$ -factor) of  $1532 \text{ MJ mm ha}^{-1} \text{ h}^{-1} \text{ yr}^{-1}$ ; 2) a soil erodibility factor ( $K$ -factor) of  $0.037 \text{ Mg ha h ha}^{-1} \text{ MJ}^{-1} \text{ mm}^{-1}$ ; 3) a cover/management factor ( $C$ -factor) of 0.21; and 4) a support practice factor ( $P$ -factor) of 1.0. The parameter settings for the Deerwood site were: 1) a  $R$ -factor of  $865 \text{ MJ mm ha}^{-1} \text{ h}^{-1} \text{ yr}^{-1}$ ; 2) a  $K$ -factor of  $0.017 \text{ Mg ha h ha}^{-1} \text{ MJ}^{-1} \text{ mm}^{-1}$ ; 3) a  $C$ -factor of 0.27; and 4) a  $P$ -factor of 1.0 (Wall et al., 2002).

### 2.3. Tillage erosion — TilLEM

Tillage erosion was estimated for the two sites using the tillage translocation model described in detail by Lobb and Kachanoski (1999). In brief, tillage translocation is simulated using a multiple linear function:

$$T_M = \alpha + \beta\theta + \gamma\varphi \quad (1)$$

where:  $T_M$  is the translocation in mass per unit width of tillage ( $\text{kg m}^{-1} \text{ pass}^{-1}$ );  $\alpha$  is the intercept of the linear regression equation, representing tillage translocation unaffected by slope gradient or slope curvature ( $\text{kg m}^{-1} \text{ pass}^{-1}$ );  $\beta$  is the coefficient for slope gradient, representing the additional tillage translocation due to slope gradient ( $\text{kg m}^{-1} \%^{-1} \text{ pass}^{-1}$ );  $\theta$  is slope gradient, positive when downslope and negative when upslope (%);  $\gamma$  is the coefficient for slope curvature, representing the additional tillage translocation due to slope curvature ( $\text{kg m}^{-1} (\%^{-1} \text{ m}) \text{ pass}^{-1}$ ); and  $\varphi$  is slope curvature, positive for convex and negative for concave ( $\% \text{ m}^{-1}$ ).

Tillage erosion is calculated as:

$$E_{Ti} = -\frac{\partial M}{\partial t} = -\frac{\partial T_M}{\partial s} = -\left(\beta \frac{\partial \theta}{\partial s} + \gamma \frac{\partial \varphi}{\partial s}\right) \quad (2)$$

where:  $E_{Ti}$  is the estimated tillage erosion, positive for soil loss and negative for soil accumulation ( $\text{kg m}^{-2} \text{ yr}^{-1}$ );  $M$  is the mass of soil per unit area above some specified base elevation ( $\text{kg m}^{-2}$ );  $t$  is time (yr); and  $s$  is the length in any specified horizontal direction (m).

Based on Eq. (2), the TilLEM, written in Visual Basic 6.0® code, was developed to calculate point-tillage-erosion rates using topographic data. Technically, the TilLEM runs on lines both parallel and perpendicular to the direction of tillage, representing forward and lateral tillage translocation, respectively. For the forward tillage translocation,  $\beta$  and  $\gamma$  were determined by previous translocation experiments. At the Deerwood site, Li et al. (in press) reported that for a full sequence of tillage operations (one pass of deep-tiller, one pass of light-cultivator followed by air-seeder and two passes of spring-tooth-harrow),  $\beta = 1.7 \text{ kg m}^{-1} \%^{-1} \text{ yr}^{-1}$  and  $\gamma = 6.4 \text{ kg m}^{-1} (\%^{-1} \text{ m}) \text{ yr}^{-1}$ . Using the tillage translocation data of Lobb et al. (1999), a sequence of one pass of mouldboard plow, two passes of tandem disc and one pass of field cultivator was estimated to have a  $\beta = 6 \text{ kg m}^{-1} \%^{-1} \text{ yr}^{-1}$  and a  $\gamma = 12 \text{ kg m}^{-1} (\%^{-1} \text{ m}) \text{ yr}^{-1}$  at the Cyrus site. For the lateral tillage translocation, the values of  $\beta$  and  $\gamma$  were assumed to be one-half of those for the forward tillage translocation (Lobb et al., 1999). The  $\beta$  and  $\gamma$  values of the Cyrus site were also used on the Deerwood site to isolate the effect of topography on tillage erosion in the comparison of the two sites.

### 2.4. Total soil erosion — $^{137}\text{Cs}$ measurements

The Mass Balance Model 2 (MBM2) in the Cs-137 Erosion Calibration Models software (Walling and He, 2001) was used to convert point- $^{137}\text{Cs}$  inventories into point-total-soil-erosion rates. The MBM2 takes into account the time-variant fallout  $^{137}\text{Cs}$  input rate and the fate of the freshly deposited fallout before it is incorporated into the till-layer by tillage. The MBM2 is generally considered superior to the proportional model and the simplified mass balance model (Walling and He, 2001; Hassouni and Bouhlassa, 2006).

For both sites, the estimated northern hemisphere annual  $^{137}\text{Cs}$  deposition flux data supplied with the software were used as the  $^{137}\text{Cs}$  fallout data (starting from 1954). The “start year of cultivation” was set at 1954, even though the actual cultivation history to 2002 is approximately 100 and 75 yrs for the Cyrus and Deerwood sites, respectively. The “mass plough depth” was calculated from the measured average  $D$  and  $\rho$  and was  $294 \text{ kg m}^{-2}$  and  $205 \text{ kg m}^{-2}$  for the Cyrus and Deerwood site, respectively. The “relaxation mass depth” ( $H_{\text{MBM2}}$ ) and the “particle size correction factor” ( $P_{\text{MBM2}}$ ) were assumed to be  $4.0 \text{ kg m}^{-2}$  and 1.0, respectively (He and Walling, 1997; Walling and He, 2001).

The proportion of annual  $^{137}\text{Cs}$  input susceptible to removal by erosion ( $\gamma_{\text{MBM2}}$ ) was estimated using the WEPP-simulated average monthly runoff pattern and the associated tillage operations. At the Cyrus site, intensive rainfall runoff events typically occur from April to September and the spring and fall tillage operations generally occur in May and October. The minimum  $\gamma_{\text{MBM2}}$  was calculated as the ratio of precipitation between May and October to the total annual precipitation (0.65). The  $\gamma_{\text{MBM2}}$  value for the Cyrus site was adjusted to 0.70 to account for spring and late-fall snowmelt runoff events. Using similar methods, the  $\gamma_{\text{MBM2}}$  value for the Deerwood site was estimated to be 0.75.

## 2.5. Statistical analysis

Model-estimated water and tillage erosion rates were determined for each DEM grid node and these points did not necessarily coincide with the sampling points. GS+5.1.1<sup>®</sup> point kriging was used to interpolate the erosion rate data onto the sampling points. To avoid smoothing, the searching radius of the interpolation was set to equal the DEM spacing, so that for a given point, data from a maximum of five closest points were used in the interpolation.

The interpolated water and tillage erosion data, the measured soil properties, crop yield and the <sup>137</sup>Cs estimated total soil erosion of the sampling points were examined with SAS 9.0<sup>®</sup>. Pearson correlation coefficients (*r*) were used to indicate the correlations between different variables (SAS Inst., 2002). The significance of *r* was grouped into three categories, i.e.  $P \leq 0.10$ ,  $\leq 0.01$ ,  $\leq 0.001$ , and were denoted using †, \*\* and \*\*\*, respectively.

For the Cyrus site, a Principal Component Analysis (PCA) was carried out in CANOCO 4.5 (ter Braak and Šmilauer, 2002) and was used to summarize variable inter-correlations and to determine the underlying data structure (Kenkel, 2006). Prior to the PCA, all data were log-transformed (except for pH) and standardized as suggested by Kenkel (2006). The superiority of the PCA to the correlation analyses was that the PCA took into account and summarized the major trends of all variables while the correlation analyses only dealt with a pair of variables at a time so that there were greater chances for the correlation analyses than for the PCA to be affected by the errors associated with individual variables, especially when the correlations were weak.

## 3. Results and discussion

### 3.1. The Cyrus site

#### 3.1.1. Patterns of estimated water, tillage and total erosion

At the Cyrus site, WEPP-estimated water erosion rates ranged from 0.2 to 57.5 Mg ha<sup>-1</sup> yr<sup>-1</sup>, averaged 18.8 Mg ha<sup>-1</sup> yr<sup>-1</sup> and the entire mapped field area showed soil loss (Fig. 1a). The basic pattern was that lower soil losses occurred in the upper-slope areas and higher soil losses occurred in the mid-slope and lower-slope areas, with the highest rates of soil loss located on the lower part of the knoll. WaTEM-estimated water erosion rates ranged from -127.8 to 98.2 Mg ha<sup>-1</sup> yr<sup>-1</sup> and averaged 24.9 Mg ha<sup>-1</sup> yr<sup>-1</sup> (Fig. 1b). The major patterns of WaTEM- and WEPP-estimated water erosion were similar. However, WaTEM estimated considerably greater soil loss on the upper part of the trough and the slightly concave slope towards the east, and considerably greater soil accumulation near the lower end of the trough. The reason for this was speculated to be that WaTEM captured the major convergent water flows better than the WEPP procedure used in this study since WaTEM incorporates a routing algorithm to track the routes of runoff. These noticeable differences between the WEPP and WaTEM estimations indicate that there are great deals of uncertainties associated with water erosion modeling.

TilLEM-estimated tillage erosion rates ranged from -25.6 to 44.9 Mg ha<sup>-1</sup> yr<sup>-1</sup> and averaged 1.1 Mg ha<sup>-1</sup> yr<sup>-1</sup> (Fig. 1c). The pattern, as expected, varied with the local relief, in particular with slope curvature. Overall, the total area of soil loss was approximately the same as that of soil accumulation. The highest rates of soil loss were found on the top of the knoll, which has a convex shape, and the highest rates of soil accumulation were found in the trough and on the eastern side-slope of the knoll, which are both concave in shape.

The <sup>137</sup>Cs-estimated total soil erosion rates ranged from -25.2 to 102.1 Mg ha<sup>-1</sup> yr<sup>-1</sup> and averaged 21.7 Mg ha<sup>-1</sup> yr<sup>-1</sup> (Fig. 1f). More than 90% of the mapped field area showed soil loss. The highest soil losses were located on the lower part of the knoll and the trough, while soil accumulation was mainly found in the footslope and toeslope areas. The pattern of <sup>137</sup>Cs-estimated total erosion did not agree well with the patterns of either the model-estimated tillage or water erosion, indicating that neither water or tillage erosion alone was able to explain the total soil erosion evident at this site. In addition, the patterns of water (WEPP)+tillage erosion (Fig. 1d) and water (WaTEM)+tillage erosion (Fig. 1e) did not agree well with the pattern of the <sup>137</sup>Cs estimated total erosion. The absence of wind erosion data and the errors associated with the models and <sup>137</sup>Cs estimations might partly explain these discrepancies. However, wind erosion is comparatively uniform within a small area and should not greatly affect the pattern (Pennock et al., 1999). Also the errors associated with the models and <sup>137</sup>Cs estimations primarily affect the magnitude of the estimated value, not the pattern (see the discussion of errors and uncertainties below). Therefore, a reasonable explanation for these discrepancies is that tillage and water erosion are not always additive and more complicated interactions between these two processes may exist.

#### 3.1.2. Correlation analyses

The correlation analyses for erosion estimates and soil properties at the Cyrus site (Table 2) showed that both WEPP- and WaTEM-estimated water erosion ( $E_{\text{WEPP}}$  and  $E_{\text{WaTEMW}}$ , respectively) and TilLEM-estimated tillage erosion ( $E_{\text{Ti}}$ ) were significantly correlated with <sup>137</sup>Cs-estimated total soil erosion ( $E_{\text{Cs}}$ ). The *r*-value of  $E_{\text{Ti}}$  ( $r=0.19^{**}$ ) was significantly lower than, but still close to, the *r*-values of  $E_{\text{WEPP}}$  ( $r=0.31^{***}$ ) and  $E_{\text{WaTEMW}}$  ( $r=0.22^{***}$ ) when correlated with  $E_{\text{Cs}}$ . However, overall, the correlations were weak and each of the three models explained only a small part of the variance of the total soil erosion. These suggest that the influence of water erosion is stronger than tillage erosion at this site, but still not strong enough to dominate the total erosion pattern across the field and, therefore, both water and tillage erosion contributed to some degree to the pattern of total soil erosion at this site. No significant differences were found between  $E_{\text{WEPP}}$  and  $E_{\text{WaTEMW}}$  when correlated with  $E_{\text{Cs}}$ . The estimates of the two water erosion models were significantly correlated with each other, but the correlation ( $r=0.40^{***}$ ) was also considered to be weak given that the two models were simulating the exact same process and, therefore, in theory, they should have produced identical results. This reinforces that there is a high degree of uncertainty associated with water erosion modeling.

Table 2  
Correlation coefficients for erosion estimates and soil properties and crop yield at the Cyrus site

	$\bar{E}_{Cs}$	$\bar{E}_{Wepp}$	$\bar{E}_{WatemW}$	$\bar{E}_{Ti}$	$\bar{E}_{Wepp+Ti}$	$\bar{E}_{WatemW+Ti}$
<i>Model estimates of annual soil erosion rates</i>						
$E_{Wepp}$	0.31***					
$E_{WatemW}$	0.22***	0.40***				
$E_{Ti}$	0.19**					
$E_{Wepp+Ti}$	0.35***	0.75***		0.65***		
$E_{WatemW+Ti}$	0.31***		0.91***	0.08	0.37***	
<i>Soil properties of the surface samples (0–15 cm) and crop yield</i>						
$\rho$	-0.16**	-0.04	-0.07	0.08	0.02	-0.04
$C_{St}$	0.17**	0.17**	0.12 <sup>†</sup>	-0.02	0.12 <sup>†</sup>	0.12 <sup>†</sup>
$C_{OC}$	-0.33***	-0.23***	-0.07	-0.10 <sup>†</sup>	-0.24***	-0.12 <sup>†</sup>
$C_{IC}$	0.47***	0.17**	0.07	0.44***	0.42***	0.27***
pH	0.37***	0.24***	0.13 <sup>†</sup>	0.19**	0.31***	0.23***
Y	-0.67***	-0.32***	-0.15**	-0.45***	-0.54***	-0.35***

$n=279-288$ .

<sup>†</sup>, \*\*, \*\*\* significant at the 0.10, 0.01 and 0.001 probability levels, respectively.

The  $r$ -values of the sum of water and tillage erosion ( $E_{Wepp+Ti}$ ,  $r=0.35***$  and  $E_{WatemW+Ti}$ ,  $r=0.31***$ ), when correlated with  $E_{Cs}$ , were both greater than those of the component model estimates (i.e.  $E_{Wepp}/E_{WatemW}$  and  $E_{Ti}$ ), indicating the superiority of combining water and tillage erosion models. The correlation between  $E_{Wepp+Ti}$  and  $E_{Wepp}$  ( $r=0.75***$ ) was greater than the correlation between  $E_{Wepp+Ti}$  and  $E_{Ti}$  ( $r=0.65***$ ). The correlation between  $E_{WatemW+Ti}$  and  $E_{WatemW}$  ( $r=0.91***$ ) was much greater than the correlation between  $E_{WatemW+Ti}$  and  $E_{Ti}$  ( $r=0.08^{NS}$ ). Again, this suggests that based on these models, water erosion contributed more than tillage erosion at the Cyrus site. To avoid the effects of systematic errors associated with the model and  $^{137}Cs$  estimations, multiple-correlation analyses of  $E_{Cs}$  against both  $E_{Wepp}$  and  $E_{Ti}$ , and of  $E_{Cs}$  against both  $E_{WatemW}$  and  $E_{Ti}$  were conducted ( $r=0.37***$  and  $0.35***$ , respectively). The multiple-correlation coefficients were close to those of  $E_{Wepp+Ti}$  and  $E_{WatemW+Ti}$ , respectively. This suggests that the systematic errors were not the reason for the observed weak correlations and further suggests that possible interactions exist between the two erosion processes.

Further correlation analyses of the model estimates with the  $^{137}Cs$  estimates were conducted on each transect parallel and perpendicular to tillage direction (data not shown). The  $r$ -values of  $E_{Wepp+Ti}$  and  $E_{WatemW+Ti}$ , in general, were much greater than those of  $E_{Wepp}/E_{WatemW}$  and  $E_{Ti}$ , which again confirms that combining water and tillage erosion model provides better estimation of total soil erosion. The  $r$ -values of  $E_{Wepp}$ , in general, were considerably greater than those of  $E_{WatemW}$  for transects parallel to the tillage direction. This could be explained by the fact that the WEPP procedure used in this study accounted for the influences of tillage on the directionality of water flows and, therefore, water erosion.

The correlations between the soil properties, crop yield and erosion estimates were generally weak and some of the  $r$ -values were too low to be used alone to draw a statistical conclusion with confidence (Table 2). However, the  $r$ -values of the crop yield and soil properties versus  $E_{Cs}$  were all significant, which

suggests that soil erosion is a fundamental cause of the variations of soil properties and crop yield across the landscape. Most of the  $r$ -values of  $E_{Cs}$ , when correlated with the crop yield and soil properties, were greater than the respective  $r$ -values (absolute value) of model estimates (i.e.  $E_{Wepp}$ ,  $E_{WatemW}$  and  $E_{Ti}$ ,  $E_{Wepp+Ti}$  and  $E_{WatemW+Ti}$ ), indicating the superiority of the  $^{137}Cs$  technique (Table 2).

### 3.1.3. PCA

The PCA well summarized the variation of all the variables (Fig. 3). The first axis alone accounted for 34.0% variance and the first two axes together accounted for 50.4% variance of all the variables. It appeared that the first axis represented the effect of total soil erosion given that  $E_{Cs}$  is closely correlated with the first axis. Other than  $\rho$  and  $C_{St}$ , all the other field-measured variables scored greater than 0.50 on the first axis and were closely correlated with  $E_{Cs}$ , indicating that the variations of these variables across the landscape were strongly affected by the pattern of total soil erosion, which confirms that total soil erosion is a fundamental cause of the variations of these variables across the landscape.

The second axis differentiated the effects of water and tillage erosion given that both  $E_{Wepp}$  and  $E_{WatemW}$  scored negatively but  $E_{Ti}$  scored positively on the second axis although  $E_{Wepp}$  and  $E_{WatemW}$  were not closely correlated (Fig. 3). The large discrepancies existed between  $E_{Wepp}$  and  $E_{WatemW}$  and between  $E_{Wepp+Ti}$  and  $E_{WatemW+Ti}$  indicate the high uncertainties associated with water erosion modeling. It is noteworthy, however,  $E_{Wepp+Ti}$  was strongly and closely correlated with  $E_{Cs}$ , suggesting that combining water and tillage erosion models was able to estimate the total soil erosion observed in the field better than their component models on their own and that at the Cyrus site, the WEPP procedure is better than the WaTEM to be used for water erosion estimation.

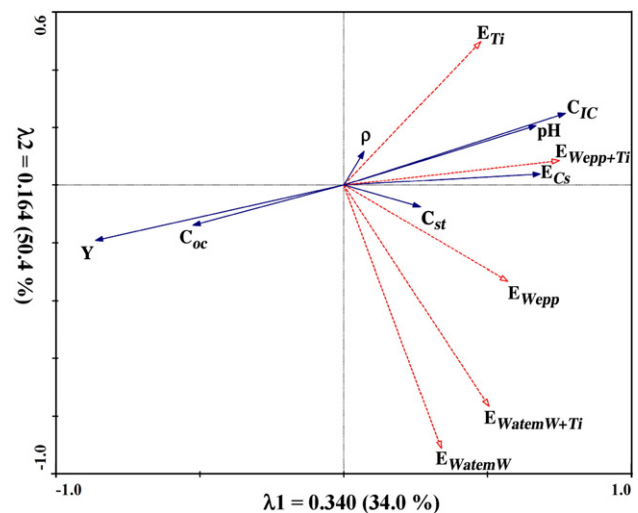


Fig. 3. Principal components analysis biplot of the data at the Cyrus site. Field-measured variables are indicated by vectors with solid lines and solid arrowheads; Model-estimated erosion variables are indicated by vectors with dashed lines and open arrowheads. Eigenvalues ( $\lambda_1$  and  $\lambda_2$  for the first and second axis, respectively) are standardized to 1.000 and the cumulative percentage variance of each axis is shown in the following bracket.

With respect to the impacts of water versus tillage erosion,  $C_{OC}$ ,  $C_{IC}$ , pH and Y were strongly and closely correlated with  $E_{W_{epp}+T_i}$ , indicating that they were influenced by both water and tillage erosion.  $C_{St}$  was more closely correlated with  $E_{W_{epp}}$  than with  $E_{T_i}$  while  $\rho$  was the opposite but the correlations were not strong.

### 3.2. The Deerwood site

#### 3.2.1. Patterns of the estimated water, tillage and total erosion

At the Deerwood site, the WEPP-estimated water erosion rates ranged from  $-1.6$  to  $8.4 \text{ Mg ha}^{-1} \text{ yr}^{-1}$  and averaged  $1.9 \text{ Mg ha}^{-1} \text{ yr}^{-1}$  (Fig. 2a). About 70% of the mapped field area showed soil loss between 0 and  $3 \text{ Mg ha}^{-1} \text{ yr}^{-1}$ , while the bottom of the bowl (depression) showed soil accumulation. The pattern of the WaTEM estimates (Fig. 2b) was similar to that of the WEPP estimates, except that WaTEM estimated soil loss over the entire mapped field area, including the depression area. Compared to the Cyrus site, estimated water-induced soil loss at the Deerwood site was considerably lower. The primary reason for this is due to the shorter slope lengths at the Deerwood site (Figs. 1, 2). The TILLEM-estimated tillage erosion rates ranged from  $-6.5$  to  $14.5 \text{ Mg ha}^{-1} \text{ yr}^{-1}$  and averaged  $2.2 \text{ Mg ha}^{-1} \text{ yr}^{-1}$  with the highest soil losses at the top of the ridge and soil accumulation in the bowl area (Fig. 2c). In comparison to the three models, the  $^{137}\text{Cs}$ -estimated total soil erosion rates ranged from  $-27.5$  to  $42.0 \text{ Mg ha}^{-1} \text{ yr}^{-1}$  and averaged  $12.1 \text{ Mg ha}^{-1} \text{ yr}^{-1}$  (Fig. 2f).

The patterns of the  $^{137}\text{Cs}$ -estimated total soil erosion, water (WEPP)+tillage erosion (Fig. 2d) and water (WaTEM)+tillage erosion (Fig. 2e) were all more similar to that of tillage erosion than that of water erosion. This suggests that tillage erosion is the dominant erosion process at the Deerwood site. The large discrepancy between the model and  $^{137}\text{Cs}$  estimates suggests that there might be systematic errors in the models. These errors were likely caused by the absence of data relating to the historically used heavier tillage implements and the low accuracy of the climate data. With the use of the Cyrus climate, management and soil data, the WEPP-estimated water erosion

( $E_{W_{epp}C}$ ) and the TILLEM-estimated tillage erosion ( $E_{T_{iC}}$ ) showed patterns almost identical to that of  $E_{W_{epp}}$  and  $E_{T_i}$ , respectively (maps not shown). The data range of the combined model ( $E_{W_{epp}C+T_{iC}}$ ) ( $-17.5$  to  $66.2 \text{ Mg ha}^{-1} \text{ yr}^{-1}$  and averaged  $12.4 \text{ Mg ha}^{-1} \text{ yr}^{-1}$ ), were close to the range of  $E_{C_s}$ , suggesting that the climate and management data from the Cyrus site might be more realistic than the generated climate and management data used at the Deerwood site.

#### 3.2.2. Correlation analyses

Correlation analyses provided further evidence that tillage erosion is the dominant erosion process at the Deerwood site (Table 3). For example: 1)  $E_{T_i}$  was significantly correlated with  $E_{C_s}$  ( $r=0.56^{***}$ ); 2) the  $r$ -values of  $E_{W_{epp}}$  ( $r=0.30^\dagger$ ) and  $E_{W_{atemW}}$  ( $r=-0.20^{NS}$ ) were significantly lower than that of  $E_{T_i}$ , when correlated with  $E_{C_s}$ ; 3) the combined models,  $E_{W_{epp}+T_i}$  and  $E_{W_{atemW}+T_i}$ , had  $r$ -values ( $r=0.59^{***}$  and  $0.49^{***}$ , respectively) which are similar to that of  $E_{T_i}$ , when correlated with  $E_{C_s}$ ; 4) the correlations determined for  $E_{W_{epp}+T_i}$  and  $E_{T_i}$  ( $r=0.94^{***}$ ) and for  $E_{W_{atemW}+T_i}$  and  $E_{T_i}$  ( $r=0.92^{***}$ ) were very strong and the  $r$ -values were considerably larger than those between  $E_{W_{epp}+T_i}$  and  $E_{W_{epp}}$  ( $r=0.55^{***}$ ) and between  $E_{W_{atemW}+T_i}$  and  $E_{W_{atemW}}$  ( $r=0.17^{NS}$ ), respectively; and 4)  $D$  and  $C_{St}$  were significantly correlated with  $E_{T_i}$  ( $r=-0.24^\dagger$  and  $0.39^{**}$ , respectively).

Similar to the Cyrus site,  $E_{W_{epp}}$  and  $E_{W_{atemW}}$  were significantly correlated ( $r=0.51^{***}$ ) but the correlation was not that strong and the uncertainties associated with water erosion modeling were considered to be high (Table 3). The strong correlations found between  $E_{W_{epp}}$  and  $E_{W_{epp}C}$  ( $r=0.94^{***}$ ), between  $E_{T_i}$  and  $E_{T_{iC}}$  ( $r=0.97^{***}$ ) and between  $E_{W_{epp}+T_i}$  and  $E_{W_{epp}C+T_{iC}}$  ( $r=0.98^{***}$ ) suggest that at the Deerwood site, the patterns of the model estimates were not sensitive to the input climate, management and soil data and, therefore, were considered largely determined by the topographic data.

For the transect data, correlation analyses of model estimates against  $^{137}\text{Cs}$  estimates also demonstrated the dominant effect of tillage erosion (data not shown). The  $r$ -values of  $E_{T_i}$  were generally much greater than the respective  $r$ -values of

Table 3  
Correlation coefficients for erosion estimates and soil properties at the Deerwood site

	$E_{C_s}$	$E_{W_{epp}}$	$E_{W_{atemW}}$	$E_{W_{epp}C}$	$E_{T_i}$	$E_{T_{iC}}$	$E_{W_{epp}+T_i}$	$E_{W_{atemW}+T_i}$	$E_{W_{epp}C+T_{iC}}$
<i>Model estimates of annual soil erosion rates</i>									
$E_{W_{epp}}$	0.30 <sup>†</sup>								
$E_{W_{atemW}}$	-0.20	0.51 <sup>***</sup>							
$E_{W_{epp}C}$	0.13	0.94 <sup>***</sup>	0.66 <sup>***</sup>						
$E_{T_i}$	0.56 <sup>***</sup>								
$E_{T_{iC}}$	0.65 <sup>***</sup>				0.97 <sup>***</sup>				
$E_{W_{epp}+T_i}$	0.59 <sup>***</sup>	0.55 <sup>***</sup>		0.44 <sup>***</sup>	0.94 <sup>***</sup>	0.95 <sup>***</sup>			
$E_{W_{atemW}+T_i}$	0.49 <sup>***</sup>		0.17		0.92 <sup>***</sup>		0.95 <sup>***</sup>		
$E_{W_{epp}C+T_{iC}}$	0.62 <sup>***</sup>	0.58 <sup>***</sup>		0.49 <sup>***</sup>		0.96 <sup>***</sup>	0.98 <sup>***</sup>		
<i>Soil properties of the surface samples (Ap horizon)</i>									
$D$	-0.48 <sup>***</sup>	0.15	0.16	0.26 <sup>†</sup>	-0.24 <sup>†</sup>	-0.23 <sup>†</sup>	-0.16	-0.18	-0.13
$\rho$	-0.23 <sup>†</sup>	0.01	0.25 <sup>†</sup>	0.05	-0.04	-0.05	-0.03	0.06	-0.03
$C_{St}$	0.43 <sup>***</sup>	0.26 <sup>†</sup>	0.06	0.29 <sup>†</sup>	0.39 <sup>**</sup>	0.45 <sup>***</sup>	0.43 <sup>***</sup>	0.42 <sup>***</sup>	0.49 <sup>***</sup>

$n=63$ .

†, \*\*, \*\*\* significant at the 0.10, 0.01 and 0.001 probability levels, respectively.

$E_{\text{Wepp}}$  and  $E_{\text{WatemW}}$  and were close to the respective  $r$ -values of  $E_{\text{Wepp}+\text{Ti}}$  and  $E_{\text{WatemW}+\text{Ti}}$ . For transects parallel to the tillage direction, the  $r$ -values of  $E_{\text{Wepp}}$  again were found to be considerably greater than those of  $E_{\text{WatemW}}$ , suggesting the existence of the directionality of water erosion induced by tillage operations.

### 3.3. Errors and uncertainties

#### 3.3.1. Errors and uncertainties associated with WEPP and WaTEM

Inaccuracy of the climate, soil, management (i.e. tillage, crop rotation) and topographic data may have all contributed errors to the water erosion model estimates. For both WEPP and WaTEM, the patterns of the estimated water erosion were largely determined by the topography. The effects of the climate, soil and management data on the estimated water erosion rates were expected to be large in the lower-slope. However, the use of Cyrus site's climate, soil and management data on the Deerwood site and a sensitivity test of WaTEM (data not shown) demonstrated that the general patterns of the estimated water erosion were not sensitive to different climate and management inputs. Tests at the Cyrus site also showed that WEPP output was not sensitive to the alteration of the three major soil types. In addition, the alteration of  $K$ -factor values in WaTEM did not make noticeable changes on the pattern of the estimated water erosion (data not shown).

A test was conducted to run the WaTEM at the Cyrus site by keeping all the other parameters the same but using the "Nearing-(rill = interrill)" routing algorithm ( $E_{\text{WatemW1}}$ ) and using a different  $k_{\text{Tc}}$  value ( $E_{\text{WatemW2}}$ ). With different routing algorithms,  $E_{\text{WatemW}}$  and  $E_{\text{WatemW1}}$  has a correlation coefficient of 0.59; with different  $k_{\text{Tc}}$  values,  $E_{\text{WatemW}}$  and  $E_{\text{WatemW2}}$  has a correlation coefficient of 0.76 and with both different routing algorithms and different  $k_{\text{Tc}}$  values  $E_{\text{WatemW1}}$  and  $E_{\text{WatemW2}}$  has a correlation coefficient of as low as 0.24 (Table 4). These indicate that WaTEM-estimated water erosion were very sensitive to different routing algorithms and the  $k_{\text{Tc}}$  values. However, after the removal of the soil accumulation data points (18–33 points out of 288 points) from the correlation analyses, the correlation coefficients between the WaTEM estimates were greatly improved and the correlation coefficients between the WaTEM estimates and WEPP estimates were also improved (Table 4). The fact that the correlation coefficient between  $E_{\text{WatemW1}}$  and  $E_{\text{WatemW2}}$  increased from 0.24 to 0.89 after the removal of soil accumulation data points indicates that using different routing-algorithms and  $k_{\text{Tc}}$  values, WaTEM predicts substantially different patterns on soil accumulation positions but the patterns on soil loss positions remains almost unchanged. An explanation for this is that WaTEM keeps track on the route of the runoff so that with different routing algorithms, towards the end of the route (e.g. in lower slope areas), a given point may have very different upslope catchment areas and with different  $k_{\text{Tc}}$  values, a given point towards the end of the route could either be a soil loss point, when the  $k_{\text{Tc}}$  value was set high, or a soil accumulation point, when the  $k_{\text{Tc}}$  value was set low.

Table 4

Correlation coefficients for water erosion model estimates at the Cyrus site

	$E_{\text{Wepp}}$	$E_{\text{WatemW}}^{\text{a}}$	$E_{\text{WatemW1}}^{\text{b}}$
<i>All data points (n = 288)</i>			
$E_{\text{WatemW}}^{\text{a}}$	0.40		
$E_{\text{WatemW1}}^{\text{b}}$	0.32	0.59	
$E_{\text{WatemW2}}^{\text{c}}$	0.45	0.76	0.24
<i>Soil accumulation data points deleted (n is indicated in brackets)</i>			
$E_{\text{WatemW}}^{\text{a}}$	0.48 (270)		
$E_{\text{WatemW1}}^{\text{b}}$	0.66 (255)	0.90 (255)	
$E_{\text{WatemW2}}^{\text{c}}$	0.47 (281)	0.98 (270)	0.89 (255)

<sup>a</sup> Using the "Govers-(1991)" routing algorithm and  $k_{\text{Tc}} = 170$  m.

<sup>b</sup> Using the "Nearing-(rill = interrill)" routing algorithm and  $k_{\text{Tc}} = 170$  m.

<sup>c</sup> Using the "Govers-(1991)" routing algorithm and  $k_{\text{Tc}} = 250$  m.

Overall, the major patterns of both WEPP- and WaTEM-estimated water erosion in this study were similar (Figs. 1, 2 and Tables 2, 3). However, the fact that large discrepancies existed between  $E_{\text{Wepp}}$  and  $E_{\text{WatemW}}$ , indicates that there are still high uncertainties associated with water erosion modeling, especially on positions that may subject to water-induced soil accumulation. There was no enough evidence to conclude that one model is in general superior to the other. However, it appeared that WaTEM captured the major water flows better, while the WEPP procedure was better able to account for the tillage-induced directionality of water erosion. For the purpose of accurate estimation of erosion rates, to choose an optimal model and to obtain accurate parameters are both important.

#### 3.3.2. Errors and uncertainties associated with Tillem

Compared to water erosion, tillage erosion is relatively simple to model. The magnitude of the estimated tillage erosion varies across the landscape as a result of only two coefficients,  $\beta$  and  $\gamma$ . The estimated tillage erosion rates were affected by both the values of  $\beta$  and  $\gamma$ . Based on previous research, the estimated tillage erosion rate was expected to be more sensitive to  $\beta$  (Lobb et al., 1999). However, as evident by using the Cyrus site's coefficients at the Deerwood site, the pattern of estimated tillage erosion was not sensitive to  $\beta$  and  $\gamma$ . WaTEM also provides a tillage erosion model, but this model does not account for the effect of the variation of slope curvature (i.e.  $\gamma = 0$ ) and, therefore, was not used in this study. Nonetheless, a test with the Cyrus data showed that the WaTEM estimates (data not shown) were very similar to the Tillem estimates ( $r = 0.89$ ), which confirms that the uncertainties associated with tillage erosion modeling are low.

#### 3.3.3. Errors and uncertainties associated with $^{137}\text{Cs}$ conversion models

Other than the MBM2, the same software used in this study provides other models to convert  $^{137}\text{Cs}$  inventory to soil erosion rates: a proportional model (PM), a simplified mass balance model (MBM1) and a more complicated mass balance model (MBM3) (Walling and He, 2001). The MBM2 used in this study is more sophisticated than the more widely used PM and

MBM1, but it requires more data inputs (i.e.  $\gamma_{\text{MBM2}}$ ,  $P_{\text{MBM2}}$  and  $H_{\text{MBM2}}$ ). Calculating  $\gamma_{\text{MBM2}}$  using the averaged climate data, assuming that  $P_{\text{MBM2}}$  was equal to 1.0 and taking  $H_{\text{MBM2}}$  values from the literature were unavoidable simplifications. Further field experiments are needed to obtain more accurate measurements of  $\gamma_{\text{MBM2}}$ ,  $P_{\text{MBM2}}$  and  $H_{\text{MBM2}}$ . A sensitivity analysis showed that the output total erosion rates were sensitive to both  $\gamma_{\text{MBM2}}$  and  $P_{\text{MBM2}}$ , but not  $H_{\text{MBM2}}$ . However, within reasonable  $\gamma_{\text{MBM2}}$  and  $P_{\text{MBM2}}$  ranges, the output varied by no more than 10%. Therefore, the accuracy of these parameters was considered to be sufficient in this study.

Another input parameter, and potential source of error was the reference  $^{137}\text{Cs}$  level used in this study. It was difficult to obtain an accurate value of the reference  $^{137}\text{Cs}$  level due to the fact that ideal reference sites are rare. The measured reference  $^{137}\text{Cs}$  level at the Deerwood site had a coefficient of variation of 9.3%. Nonetheless, the measured  $^{137}\text{Cs}$  levels at both reference sites used this study were comparable to those reported by other researchers in the northern NAGP (e.g. de Jong et al., 1983; Pennock et al., 1999). In addition, the errors associated with the reference  $^{137}\text{Cs}$  level primarily cause a shift between soil loss and accumulation, however, the relative differences remain constant and, therefore, will not affect the results of the correlation analyses.

A test with the Cyrus site data showed that the soil erosion pattern estimated using the PM was very similar to that estimated using MBM2 ( $r=0.95$ ) and the actual values of the PM estimates (averaged  $25.7 \text{ Mg ha}^{-1} \text{ yr}^{-1}$ ) were close to those of the MBM2 estimates (averaged  $21.4 \text{ Mg ha}^{-1} \text{ yr}^{-1}$ ). The patterns of MBM1 and MBM2 estimates were almost identical ( $r=1.00$ ). However, the actual values of the MBM1 estimates (averaged  $46.2 \text{ Mg ha}^{-1} \text{ yr}^{-1}$ ) were substantially different from those of the MBM2 estimates. This suggests that the errors and uncertainties of the estimated soil erosion pattern are low but the errors and uncertainties of the estimated soil erosion rates might be high. Caution should be taken for the use of MBM1 when the goal is to obtain accurate soil erosion rates not an accurate pattern of soil erosion across the landscape. In the case of the Cyrus site, the PM appears to be a better alternative than MBM1 when the parameterization for MBM2 is difficult. The MBM3 incorporates a two-dimensional tillage erosion model, which does not take into account lateral translocation and the effect of changing slope curvature (i.e.  $\gamma=0$ ), and, therefore, might not be suitable for topographically complex landscapes (Walling and He, 2001).

#### 4. Conclusions

Patterns of water and tillage erosion are fundamentally different within topographically complex landscapes. Total soil erosion, which is an integrated result of individual erosion processes and their interactions, can be well estimated using the  $^{137}\text{Cs}$  technique. Water and tillage erosion models tested alone provide acceptable estimation of total soil erosion only when that process is dominant over the other process(es). Combining water and tillage erosion models generally provided a better estimation of total soil erosion than the component models on their own.

The contributions of water and tillage erosion towards the total soil erosion vary in different landscapes. On the slope of undulating landscapes, tillage and water erosion both contribute considerably to total soil erosion. Neither water nor tillage erosion dominates over the other erosion process and the interactions between these two erosion processes may be strong. On the knoll of hummocky landscapes, tillage erosion dominates the pattern of total soil erosion and the effects of water erosion are minor.

Soil erosion was found to be a fundamental cause of the variation of soil properties and crop yield across the landscape. Most soil properties and crop yield were found to be closely correlated with total soil erosion.

Great uncertainties were found associated with water erosion models, especially for soil accumulation estimations. Uncertainties associated with tillage erosion model and the  $^{137}\text{Cs}$  conversion models were relatively low. Overall, the estimated patterns remained similar to each other when tested with different models and when the parameters used were in reasonable ranges. However, it was necessary to choose an optimal model and to obtain accurate parameters for the purpose of accurate assessments of soil erosion rates.

#### Nomenclature

$C$ -factor	cover/management factor (dimensionless ratio)
$C_{\text{IC}}$	soil inorganic carbon (carbonates) content (%)
$C_{\text{OC}}$	soil organic carbon content (%)
$C_{\text{St}}$	stone content (%)
$D$	depth of the Ap horizon (m)
$E_{\text{Cs}}$	$^{137}\text{Cs}$ estimated total soil erosion, positive for soil loss, negative for soil accumulation ( $\text{Mg ha}^{-1} \text{ yr}^{-1}$ )
$E_{\text{Ti}}$	Tillem estimated tillage erosion, positive for soil loss, negative for soil accumulation ( $\text{Mg ha}^{-1} \text{ yr}^{-1}$ )
$E_{\text{TiC}}$	Tillem estimated tillage erosion on the Deerwood site using the Cyrus site's tillage erosivity data, positive for soil loss, negative for soil accumulation ( $\text{Mg ha}^{-1} \text{ yr}^{-1}$ )
$E_{\text{WaterW}}$	WaTEM estimated water erosion, positive for soil loss, negative for soil accumulation ( $\text{Mg ha}^{-1} \text{ yr}^{-1}$ )
$E_{\text{WaterW} + \text{Ti}}$	the sum of WaTEM estimated water erosion and Tillem estimated tillage erosion, positive for soil loss, negative for soil accumulation ( $\text{Mg ha}^{-1} \text{ yr}^{-1}$ )
$E_{\text{Wepp}}$	WEPP estimated water erosion, positive for soil loss, negative for soil accumulation ( $\text{Mg ha}^{-1} \text{ yr}^{-1}$ )
$E_{\text{WeppC}}$	WEPP estimated water erosion on the Deerwood site using the Cyrus site's climate, management and soil data, positive for soil loss, negative for soil accumulation ( $\text{Mg ha}^{-1} \text{ yr}^{-1}$ )
$E_{\text{Wepp} + \text{Ti}}$	the sum of WEPP estimated water erosion and Tillem estimated tillage erosion, positive for soil loss, negative for soil accumulation ( $\text{Mg ha}^{-1} \text{ yr}^{-1}$ )
$E_{\text{WeppC} + \text{TiC}}$	the sum of WEPP estimated water erosion and Tillem estimated tillage erosion on the Deerwood site using the Cyrus site's climate, management, soil and tillage erosivity data, positive for soil loss, negative for soil accumulation ( $\text{Mg ha}^{-1} \text{ yr}^{-1}$ )
$H_{\text{MBM2}}$	the relaxation mass depth of the initial distribution of fallout $^{137}\text{Cs}$ in the soil profile used in MBM2 ( $\text{kg m}^{-2}$ )
$K$ -factor	soil erodibility factor ( $\text{Mg ha h ha}^{-1} \text{ MJ}^{-1} \text{ mm}^{-1}$ )

$k_{Tc}$	Transport capacity coefficient used in WaTEM (m)
$M$	the mass of soil per unit area above a specified base elevation ( $\text{kg m}^{-2}$ )
MBM1	Mass Balance Model 1 in the Cs-137 Erosion Calibration Models software
MBM2	Mass Balance Model 2 in the Cs-137 Erosion Calibration Models software
MBM3	Mass Balance Model 3 in the Cs-137 Erosion Calibration Models software
NAGP	North American Great Plains
$P$ -factor	support practice factor (dimensionless ratio)
PCA	Principal Components Analysis
PM	Proportional Model in the Cs-137 Erosion Calibration Models software
$P_{\text{MBM2}}$	particle size correction factor used in MBM2 (dimensionless ratio)
$R$ -factor	rainfall-runoff erosivity factor ( $\text{MJ mm ha}^{-1} \text{h}^{-1} \text{yr}^{-1}$ )
RUSLE	Revised Universal Soil Loss Equation
$s$	the length in any specified horizontal direction (m)
$t$	time (yr)
TilLEM	Tillage Erosion Model
WaTEM	Water and Tillage Erosion Model
WEPP	Water Erosion Prediction Project
$Y$	Four-year (from 2000 to 2003) averaged crop yield at the Cyrus site
$\alpha$	the intercept of the linear regression equation, representing tillage translocation unaffected by slope gradient or slope curvature and indicating the dispersivity of the given tillage operation ( $\text{kg m}^{-1} \text{pass}^{-1}$ )
$\beta$	the coefficient for slope gradient, representing the extra tillage translocation due to slope gradient and indicating the erosivity of the given tillage operation ( $\text{kg m}^{-1} \%^{-1} \text{pass}^{-1}$ )
$\gamma$	the coefficient for slope curvature, representing the extra tillage translocation due to slope curvature and indicating the erosivity of the given tillage operation ( $\text{kg m}^{-1} (\%^{-1} \text{m}) \text{pass}^{-1}$ )
$\gamma_{\text{MBM2}}$	the proportion of the annual $^{137}\text{Cs}$ input susceptible to removal by erosion used in the MBM2 model (dimensionless ratio)
$\varphi$	slope curvature, positive for convex and negative for concave ( $\% \text{m}^{-1}$ )
$\lambda 1$	Eigenvalue of the first axis in the PCA biplot
$\lambda 2$	Eigenvalue of the second axis in the PCA biplot
$\theta$	slope gradient, positive when downslope and negative when upslope ( $\%$ )
$\rho$	dry soil bulk density ( $\text{kg m}^{-3}$ )

## Acknowledgements

Financial support for this study was provided by Natural Sciences and Engineering Research Council of Canada (NSERC) as part of project STPGP 246185-01 entitled “Tillage erosion and its impacts on soil characteristics and pesticide fate processes at the large-scale” project. The authors would like to thank Dr. K. Van Oost for the help of WaTEM application and K. Tiessen for reviewing an earlier draft of

this manuscript. The authors gratefully acknowledge the anonymous reviewers for their constructive comments and suggestions.

## References

- De Alba, S., Lindstrom, M.J., Schumacher, T.E., Malo, D.D., 2004. Soil landscape evolution due to soil redistribution by tillage: a new conceptual model of soil catena evolution in agricultural landscapes. *Catena* 58, 77–100.
- de Jong, E., Begg, C.B.M., Kachanoski, R.G., 1983. Estimates of soil erosion and deposition for some Saskatchewan soils. *Can. J. Soil Sci.* 63, 607–617.
- Desmet, P.J.J., Govers, G., 1997. Two-dimensional modeling of the within-field variation in rill and gully geometry and location related to topography. *Catena* 19, 283–306.
- Environment Canada, 2006. Canadian Climate Normals or Averages 1971–2000 [Online]. Available at: [http://www.climate.weatheroffice.ec.gc.ca/climate\\_normals/index\\_e.html](http://www.climate.weatheroffice.ec.gc.ca/climate_normals/index_e.html).
- Flanagan, D.C., Nearing, M.A. (Eds.), 1995. USDA-Water Erosion Prediction project: Hillslope profile and watershed model documentation. NSERL Report, vol. 10. USDA-ARS National Soil Erosion Research Laboratory, West Lafayette, IN. 47097-1196.
- Govers, G., Vandaele, K., Desmet, P.J.J., Poesen, J., Bunte, K., 1994. The role of tillage in soil redistribution on hillslopes. *Eur. J. Soil Sci.* 45, 469–478.
- Hassouni, K., Bouhlassa, S., 2006. Estimation of soil erosion on cultivated soils using  $^{137}\text{Cs}$  measurements and calibration models: a case study from Nakhla watershed, Morocco. *Can. J. Soil Sci.* 86, 77–87.
- He, Q., Walling, D.E., 1997. The distribution of fallout  $^{137}\text{Cs}$  and  $^{210}\text{Pb}$  in undisturbed and cultivated soils. *Appl. Radiat. Isotopes* 48, 677–690.
- Heuvelink, G.B.M., Schoorl, J.M., Veldkamp, A., Pennock, D.J., 2006. Space-time Kalman filtering of soil redistribution. *Geoderma* 133, 124–137.
- Jetten, V., Govers, G., Hessel, R., 2003. Erosion models: quality of spatial predictions. *Hydrol. Process.* 17, 887–900.
- Kenkel, N.C., 2006. On selecting an appropriate multivariate analysis. *Can. J. Plant Sci.* 86, 663–676.
- Li, S., Lobb, D.A., Lindstrom, M.J., in press. Tillage translocation and tillage erosion in cereal-based production in Manitoba, Canada. *Soil Tillage Res.* doi:10.1016/j.still.2006.07.019.
- Lindstrom, M.J., Nelson, W.W., Schumacher, T.E., Lemme, G.D., 1990. Soil movement by tillage as affected by slope. *Soil Tillage Res.* 17, 255–264.
- Lindstrom, M.J., Nelson, W.W., Schumacher, T.E., 1992. Quantifying tillage erosion rates due to moldboard plowing. *Soil Tillage Res.* 24, 243–255.
- Lobb, D.A., 1991. Soil erosion processes on shoulder slope landscape positions. M.Sc. Thesis. University of Guelph. Guelph. 390 pp.
- Lobb, D.A., Kachanoski, R.G., 1999. Modelling tillage erosion in topographically complex landscapes of southwestern Ontario, Canada. *Soil Tillage Res.* 51, 261–278.
- Lobb, D.A., Kachanoski, R.G., Miller, M.H., 1995. Tillage translocation and tillage erosion on shoulder slope landscape positions measured using  $^{137}\text{Cs}$  as a tracer. *Can. J. Soil Sci.* 75, 211–218.
- Lobb, D.A., Kachanoski, R.G., Miller, M.H., 1999. Tillage translocation and tillage erosion in the complex upland landscapes of southwestern Ontario. *Soil Tillage Res.* 51, 189–209.
- Lobb, D.A., Lindstrom, M.J., Schumacher, T.E., 2003. Soil erosion processes and their interactions: implications for environmental indicators. In: Franca-viglia, R. (Ed.), *Agricultural Impacts on Soil Erosion and Soil Biodiversity: Developing Indicators for Policy Analysis*. Proceedings from an OECD Expert Meeting — Rome, Italy, March, pp. 325–336.
- Loeppert, R.H., Suarez, D.L., 1996. Carbonate and gypsum. In: Bartels, J.M. (Ed.), *Methods of Soil Analysis. Part 3. Chemical Methods*. ASA/SSSA, Madison, WI, pp. 437–475.
- McKeague, J.A. (Ed.), 1978. *Manual on soil sampling and methods of analysis*. Canadian Society of Soil Science, Ottawa, Canada. 212 pp.
- Nelson, D.E., Sommers, L.E., 1982. Total carbon, organic carbon, and organic matter. In: Page, A.L. (Ed.), *Methods of Soil Analysis. Part 2. Chemical and Microbiological Properties*. ASA/SSSA, Madison, WI, pp. 539–577.
- Papiernik, S.K., Lindstrom, M.J., Schumacher, J.A., Farenshorst, A., Stephens, K.D., Schumacher, T.E., Lobb, D.A., 2005. Variation in soil properties and

- crop yield across and eroded prairie landscape. *J. Soil Water Conserv.* 60, 388–395.
- Pennock, D.J., 2003. Terrain attributes, landform segmentation, and soil redistribution. *Soil Tillage Res.* 69, 15–26.
- Pennock, D.J., Corre, M.D., 2001. Development and application of landform segmentation procedures. *Soil Tillage Res.* 58, 151–162.
- Pennock, D.J., McCann, B.L., de Jong, E., Lemmen, D.S., 1999. Effects of soil redistribution on soil properties in a cultivated Solonchic–Chernozemic landscape of southwestern Saskatchewan. *Can. J. Soil Sci.* 79, 593–601.
- Quine, T.A., Govers, G., Walling, D.E., Zhang, X., Desmet, P.J.J., Zhang, Y., Vandaele, K., 1997. Erosion processes and landform evolution on agricultural land — new perspectives from caesium-137 measurements and topographic-based erosion modelling. *Earth Surf. Processes Landf.* 22, 799–816.
- Renard, K.G., Foster, G.R., Weesies, G.A., McCool, D.K., Yoder, D.C., 2001. Predicting soil erosion by water — a guide to conservation planning with the revised universal soil loss equation (RUSLE). *Agriculture Handbook*, vol. 703. USDA-ARS, Washington, D.C.
- SAS institute, Inc., 2002. SAS® 9 Help and Documents. SAS Institute, Inc., Cary, NC 27513, USA.
- Schumacher, T.E., Lindstrom, M.J., Schumacher, J.A., Lemme, G.D., 1999. Modeling spatial variation in productivity due to tillage and water erosion. *Soil Tillage Res.* 51, 331–339.
- Schumacher, J.A., Kaspar, T.C., Ritchie, J.C., Schumacher, T.E., Karlen, D.L., Venteris, E.R., McCarty, G.W., Colvin, T.S., Jaynes, D.B., Lindstrom, M.J., Fenton, T.E., 2005. Identifying spatial patterns of erosion for use in precision conservation. *J. Soil Water Conserv.* 60, 355–362.
- Takken, I., Jetten, V., Govers, G., Nachtergaele, J., Steegen, A., 2001. The effect of tillage-induced roughness on runoff and erosion patterns. *Geomorphology* 37, 1–14.
- ter Braak, C.J.F., Šmilauer, P., 2002. *CANOCO Reference Manual and CanoDraw for Windows User's Guide: Software for Canonical Community Ordination (version 4.5)*. Microcomputer Power, Ithaca, NY, USA. 500 pp.
- Van Oost, K., Govers, G., Desmet, P., 2000. Evaluating the effects of changes in landscape structure on soil erosion by water and tillage. *Landscape Ecol.* 15, 577–589.
- Wall, G.J., Coote, D.R., Pringle, E.A., Shelton, I.J. (Eds.), 2002. *RUSLEFAC — Revised Universal Soil Loss Equation for Application in Canada: A Handbook for Estimating Soil Loss from Water Erosion in Canada*. Research Branch, Agriculture and Agri-Food Canada, Ottawa. Contribution No. 02-92. 117 pp.
- Walling, D.E., He, Q., 2001. Models for converting  $^{137}\text{Cs}$  measurements to estimates of soil redistribution rates on cultivated and uncultivated soils, and estimating bomb-derived  $^{137}\text{Cs}$  reference inventories (including software for model implementation). A Contribution to the IAEA Coordinated Research Programmes on Soil Erosion (D1.50.05) and Sedimentation (F3.10.01).